J|A|C|S ARTICLES

Published on Web 11/12/2009

Gigantic Enhancement in Sensitivity Using Schottky Contacted Nanowire Nanosensor

Te-Yu Wei,[†,‡] Ping-Hung Yeh,[†,§] Shih-Yuan Lu,[*,‡] and Zhong Lin Wang[*,†]

School of Materials Science and Engineering, Georgia Institute of Technology, Atlanta, Georgia 30332, Department of Chemical Engineering, National Tsing-Hua University, Hsin-Chu, Taiwan 30013, Republic of China, and Department of Physics, Tamkang University, Tansui, Taiwan 251, Republic of China

Received September 17, 2009; E-mail: zhong.wang@mse.gatech.edu; sylu@mx.nthu.edu.tw

Abstract: A new single nanowire based nanosensor is demonstrated for illustrating its ultrahigh sensitivity for gas sensing. The device is composed of a single ZnO nanowire mounted on Pt electrodes with one end in Ohmic contact and the other end in Schottky contact. The Schottky contact functions as a "gate" that controls the current flowing through the entire system. By tuning the Schottky barrier height through the responsive variation of the surface chemisorbed gases and the amplification role played by the nanowire to Schottky barrier effect, an ultrahigh sensitivity of 32 000% was achieved using the Schottky contacted device operated in reverse bias mode at 275 °C for detection of 400 ppm CO, which is 4 orders of magnitude higher than that obtained using an Ohmic contact device under the same conditions. In addition, the response time and reset time have been shortened by a factor of 7. The methodology and principle illustrated in the paper present a new sensing mechanism that can be readily and extensively applied to other gas sensing systems.

Introduction

For high sensitive substance sensing, nanodevices based on one-dimensional (1D) nanostructures, including nanowires,[1−6] nanobelts,[7,8] and nanotubes,[9−12] have shown great promise because of their advantageous large surface to volume ratio and finite, readily manipulative charge carrier flow of the confined charge transport channel. Most, if not all, of these 1D nanostructure based nanodevices are composed of a functional single nanowire (NW) mounted at its two ends on electrodes to form a field effect transistor (FET). The two contact ends of the device are usually designed to have Ohmic contacts to largely enhance the contribution to conductance from the NW and minimize the resistance of charge carrier flow across the contacts because the mechanism of the sensor is about the change in conductance of the device once it is exposed to the species to be detected, which are expected to change the surface conductance of the NW due to modification of the surface charge and states, disturbance of the gate potential, and change in local band alignment and/or permittivity. For gas sensing, past research efforts to improve the sensitivity have focused on new material growth processes,[13,14] networking of the functional material,[15,16] and surface modification of the functional material with polymer or nanoparticles.[17−20]

Recently, our group has demonstrated that Schottky contact can largely improve the sensitivity of nanowire nanosensors for detecting UV and biologically and chemically charged molecules.[21,22] The core of the device relies on the nonsymmetrical Schottky contact under reverse bias, which has been demonstrated to enhance the sensitivity by several orders of magnitude. In this

[†] Georgia Institute of Technology.
[‡] National Tsing-Hua University.
[§] Tamkang University.

(1) Fan, Z; Lu, J. G. *Appl. Phys. Lett.* **2005**, *86*, 123510.
(2) Cui, Y.; Wei, Q.; Park, H.; Lieber, C. M. *Science* **2001**, *293*, 1289.
(3) Wang, X.; Zhou, J.; Song, J.; Liu, J.; Xu, N.; Wang, Z. L. *Nano Lett.* **2006**, *6*, 2768.
(4) Zhang, Z.; Hu, C.; Xiong, Y.; Yang, R.; Wang, Z. L. *Nanotechnology* **2007**, *18*, 465504.
(5) Kuang, Q.; Lao, C.; Wang, Z. L.; Xie, Z.; Zheng, L. *J. Am. Chem. Soc.* **2007**, *129*, 6070.
(6) Shen, G.; Chen, P. C.; Ryu, K.; Zhou, C. *J. Mater. Chem.* **2009**, *19*, 828.
(7) Comini, E.; Faglia, G.; Sberveglieri, G.; Pan, Z.; Wang, Z. L. *Appl. Phys. Lett.* **2002**, *81*, 1869.
(8) Cheng, Y.; Xiong, P.; Yun, C. S.; Strouse, G. F.; Zheng, J. P.; Yang, R. S.; Wang, Z. L. *Nano Lett.* **2008**, *8*, 4179.
(9) Gui, E. L.; Li, L. J.; Zhang, K.; Xu, Y.; Dong, X.; Ho, X.; Lee, P. S.; Kasim, J.; Shen, Z. X.; Rpgers, J. A.; Mhaisalkar, S. G. *J. Am. Chem. Soc.* **2007**, *129*, 14427.
(10) Kauffman, D. R.; Star, A. *Angew. Chem., Int. Ed.* **2008**, *47*, 2.
(11) Zheng, Q.; Zhou, B.; Bai, J.; Li, L.; Jin, Z.; Zhang, J.; Li, J.; Liu, Y.; Cai, W.; Zhu, X. *Adv. Mater.* **2008**, *20*, 1044.
(12) Grimes, C. A. *J. Mater. Chem.* **2007**, *17*, 1451.
(13) Law, J. B. K.; Thong, J. T. L. *Nanotechnology* **2008**, *19*, 205502.
(14) Ahn, M. W.; Park, K. S.; Heo, J. H.; Park, J. G.; Kim, D. W.; Choi, K. J.; Lee, J. H.; Hong, S. H. *Appl. Phys. Lett.* **2008**, *93*, 263103.
(15) Zhou, J.; Deng, S. Z.; Xu, N. S.; Ding, Y.; Wang, Z. L. *Appl. Phys. Lett.* **2006**, *88*, 203101.
(16) Wang, Y.; Du, G.; Liu, H.; Liu, D.; Qin, S.; Wang, N.; Hu, C.; Tao, X.; Jiao, J.; Wang, J.; Wang, Z. L. *Adv. Funct. Mater.* **2008**, *18*, 1.
(17) He, J. H.; Lin, Y. H.; McConney, M. E.; Tsukruk, V. V.; Wang, Z. L.; Bao, G. *J. Appl. Phys.* **2007**, *102*, 084303.
(18) Lao, C. S.; Park, M. C.; Kuang, Q.; Deng, Y.; Sood, A. K.; Polla, D. L.; Wang, Z. L. *J. Am. Chem. Soc.* **2007**, *129*, 12096.
(19) Kuang, Q.; Lao, C. S.; Li, Z.; Liu, Y. Z.; Xie, Z. X.; Zheng, L. S.; Wang, Z. L. *J. Phys. Chem. C* **2008**, *112*, 11539.
(20) He, J. H.; Ho, C. H.; Chen, C. Y. *Nanotechnology* **2009**, *20*, 06550.
(21) Zhou, J.; Gu, Y.; Hu, Y.; Mai, W.; Yeh, P. H.; Bao, G.; Sood, A. K.; Polla, D. L.; Wang, Z. L. *Appl. Phys. Lett.* **2009**, *94*, 191103.
(22) Yeh, P. H.; Li, Z.; Wang, Z. L. *Adv. Mater.* **2009**, *21* DOI: 10.1002/adma.200902172.

 10.1021/ja907585c CCC: $40.75

work, the Schottky contacted ZnO NW nanosensor is demonstrated, which gives an enhancement in sensitivity by 4 orders of magnitude over the Ohmic contacted device in the detection of CO. The new design differs from the conventional ones by purposely introducing a Schottky contact at one of the two contacting ends of the device. The small contact area between the NW and the electrode magnifies the influence of the molecules adsorbed at the junction area on the local Schottky barrier height (SBH), which serves as a "gate" for controlling the transport of charge carriers. This offers a new approach for designing ultrasensitive NW sensors, and it can be applied to a wide range of gases and nanomaterials.

Experimental Methods

The preparation of single crystalline ZnO NWs followed the procedures presented in a pervious work.[25] Briefly, a suitable amount of ZnO powders, serving as the precursor, was loaded to an alumina boat that was placed at the center of an alumina tube of 75 cm length. The alumina tube is situated in a furnace to serve as the reaction chamber. Argon, the carrier gas, at a flow rate of 50 sccm flows through the alumina tube to transport the ZnO vapors downstream for the NW growth. The furnace was heated to 1475 °C and held at that temperature for 4.5 h under ~250 mbar. After the NW growth, the tube was cooled under an argon flow.

Ohmic contact devices (OCD) and Schottky contact devices (SCD) were fabricated by using ZnO NWs from the same production batch. For the fabrication of an OCD, a single ZnO NW was first placed on a pair of Pt pattern electrodes, and then the two ends of the NW were fixed by deposition of Pt/Ga using a focus ion beam (FIB) system (FEI Nova Nanolab 200 FIB/SEM). The resulting contact between the Pt/Ga deposit and the ZnO NW was an Ohmic contact. The length of the NW was controlled to be sufficiently long to minimize the potential contamination from the FIB operation. The fabrication of an SCD followed the same procedure, except that one end of the NW was in physical contact with the Pt electrode without the treatment using FIB. The contact thus formed between the Pt electrode and the ZnO NW was a Schottky contact, whereas the other end is an Ohmic contact through the deposition of Pt/Ga using FIB.

The gas sensing characteristics of the two types of devices, OCD and SCD, were determined via the relevant $I-V$ curve measurements conducted at different temperatures under gas atmosphere of different concentrations. The gases to be detected were O_2 and CO. The sensitivity (S) was calculated by $\Delta I/I_0$, where ΔI was the amount of current change induced after exposure of the device to the target gas atmosphere and I_0 was the initial current.

Results and Discussion

The gas sensing characteristics of the OCD toward oxygen were first investigated. Here, the O_2 atmosphere was afforded as a 10 wt % O_2 in N_2. Figure 1a shows the $I-V$ curves of the OCD recorded at 275 °C when exposed to N_2 and O_2 atmospheres. The OCD is depicted in the inset of Figure 1a. As expected, the two $I-V$ plots appeared to be linear, showing an excellent Ohmic contact characteristic. The slopes of the two lines are, however, slightly different, with the slope of the O_2 slightly smaller than that of the N_2. This translates to a slightly larger resistance associated with the O_2 case, in accord with the expected surface electron-depletion layer created by the chemisorbed oxygen species, O^-, on the ZnO NW surface. If one examines the response curve of the OCD toward sensing of O_2, one would observe a slight decrease in current values when the atmosphere is shifted from N_2 to O_2. Figure 1b shows such curves for six system temperatures, ranging from 150 to

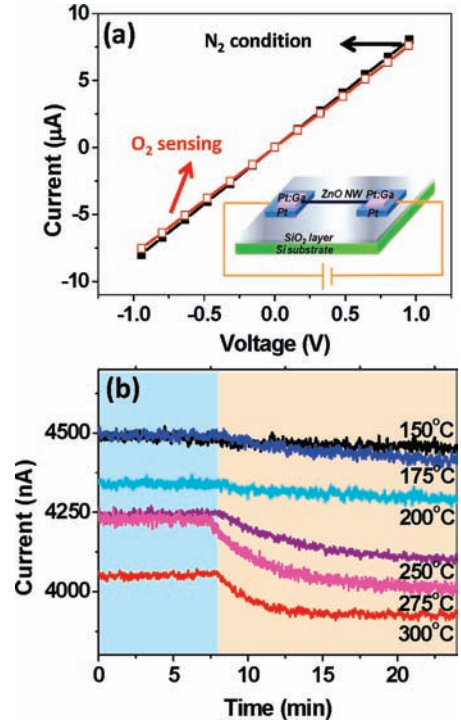

Figure 1. (a) $I-V$ curves measured for the Ohmic contact device (OCD) in N_2 and O_2 atmospheres at 275 °C. Inset shows the schematic of the OCD. (b) The response curves of the oxygen detection recorded at different temperatures, ranging from 150 to 300 °C, for the OCD. The blue background denotes that the OCD was in the N_2 atmosphere and the pink background in the O_2 atmosphere.

300 °C, and as anticipated, the current drops are rather insignificant in magnitude, corresponding to low sensitivities. Furthermore, the current responses were slow, taking several minutes to reach the new steady states. The highest sensitivity of only 4.8% was obtained at a response time of 500 s for the 275 °C case. It can be inferred that the conductance decrease acquired from the adsorption of the negatively charged oxygen ions is only very minor compared to the inherent conductance of the ZnO NW.

Also observed from Figure 1b is that the sensitivity of the OCD increases with increasing temperature and reaches a maximum at 275 °C. When the temperature is increased, the electrons become more energetic and can overcome larger transfer resistances. This is a probable reason for the sensitivity drop at temperatures from 275 to 300 °C. The response curves of Figure 1b all exhibited the exponential decay characteristic, and one can thus define a response time constant for each sensing event as the time needed to achieve a 63% deviation from the initial state, which is calculated using the time required for the current to drop to 1/e in ratio. With this parameter, one can quantify how fast the sensing response is. The response time constant thus calculated for the 275 °C case, the highest sensitivity case, was 209 s, indicating a slow sensing response and reset.

For the ZnO NW nanosensor using Ohmic contact at the two ends, the conductance of the entire device is largely determined by the NW. O_2 is a strong electron-drawing species and reduces the system conductance when adsorbed onto the surface of the ZnO NW by causing an electron-depletion layer on the surface of the NW. Once accepting electrons from the NW, the chemisorbed oxygen is turned into negatively charged species, O_2^-, O^-, or O^{2-}, depending on the system temperature.[23]

(25) Pan, Z. W.; Dai, Z. R.; Wang, Z. L. *Science* **2001**, *291*, 1947.

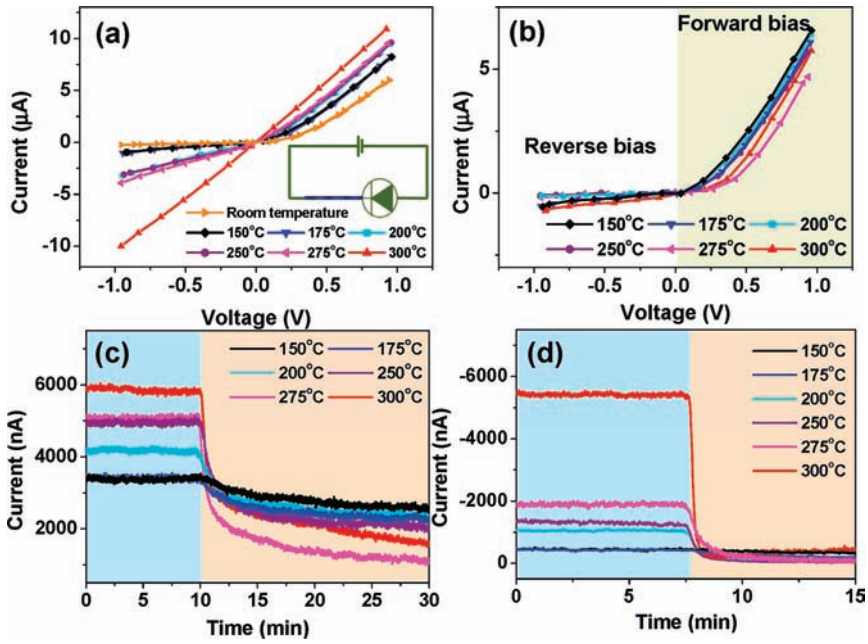

Figure 2. (a) $I-V$ curves of the Schotty contact device (SCD) measured at different temperatures in N_2 atmosphere. Inset shows the circuitry of the Schottky gated gas sensor device. (b) $I-V$ curves of the SCD measured at different temperatures in O_2 atmosphere. Different background colors are used to highlight the different operation mode, forward or reverse bias, of the device. (c) Response curves of the oxygen detection recorded at different temperatures, ranging from 150 to 300 °C, for the SCD operated at the forward bias mode. (d) Response curves of the oxygen detection recorded at different temperatures, ranging from 150 to 300 °C, for the SCD operated at the reverse bias mode.

Now let us turn to the sensing performance of the SCD toward O_2. Figure 2a shows the $I-V$ curves of the SCD measured at six different temperatures in the N_2 atmosphere. The effective circuitry of the SCD is depicted as an inset of Figure 2a. Evidently, all $I-V$ curves recorded show typical Schottky contact characteristics. The Schottky contact characteristics, however, became less pronounced with increasing system temperature. This can be attributed to the increasingly higher energies of the electrons at high temperatures, worsening the rectifying function of the Schottky contact. At a temperature of 300 °C, the $I-V$ curve became almost linear, closer to the Ohmic contact behavior.

Once the oxygen atmosphere was introduced, the conductances for both forward and reverse bias modes were decreased because of the formation of the electron-depletion layer on the ZnO NW surface. With a careful comparison of Figure 2a,b, one observes that the decreases in conductance achieved by the reverse bias mode were much more pronounced than those produced by the forward bias mode. More interestingly, the $I-V$ curves of the SCD after the oxygen adsorption exhibited much better Schottky contact characteristics than before, even at a high temperature of 300 °C. This can be attributed in part to the larger resistances induced by the formation of the electron-depletion layer, but there is more to it, as discussed in a later section. The corresponding response curves of the SCD are shown in Figure 2c,d for the forward and reverse bias modes, respectively. First, let us examine the results of the forward bias case. If one compares Figures 1b and 2c, it is evident that the current reductions caused by the SCD at forward bias (SCFD) were much larger in magnitude than those achieved with the OCD, implying much higher sensitivities for the SCFD. The highest sensitivity of 257% was obtained at the response time of 500 s and temperature of 275 °C, 54 times higher than the highest sensitivity of 4.8% achieved by the OCD under the same sensing conditions. It can also be concluded from Figure 2c that the sensitivity increased with increasing temperature and reached a maximum at 275 °C. The reason for the sensitivity drop, when further increasing the temperature to 300 °C, is the same as that for the OCD case. In terms of the response time constant, it was 62 s for the SCFD, much shorter than the 209 s of the OCD.

The sensing performance for the SCD at the reverse bias mode (SCRD) is shown in Figure 2d. First, one notices that there existed an order of magnitude difference between the currents before and after the O_2 introduction, a 2 orders of magnitude drop from 10^{-6} to 10^{-8} A to be more specific. The corresponding sensitivities are thus much higher than those of both the OCD and the SCFD. A highest sensitivity of 3235% was obtained for the SCRD at the response time of 500 s and temperature of 250 °C, and the corresponding response time constant was 30 s. The sensitivities of the SCRD decreased when the temperature was raised above 250 °C, again attributable to the effect of increasingly higher thermal energy electrons. The sensitivities of the SCRD, SCFD, and OCD measured at six different temperatures are shown and compared in Figure 4a. For the 250 °C case, the sensitivity of the SCRD was 1085 times higher than that of the OCD and 27 times higher than that of the SCFD. The response time constants followed the same trend.

The formation of the electron-depletion layer alone at the NW surface cannot account for the ultrahigh sensitivity achieved by the SCRD. Here, we propose a second, more important mechanism—the rise in SBH induced by the adsorption of the negatively charged oxygen ions, O^-, at the Schottky contact. The SBH rise significantly reduced the electron flow across the Schottky contact interface. This effect is much more pronounced for the reverse bias mode than for the forward bias mode since the electrons need to overcome the Schottky barrier to form

(23) Chaabouni, F.; Abaab, M.; Rezig, B. *Sens. Actuators, B* **2004**, *100*, 200.

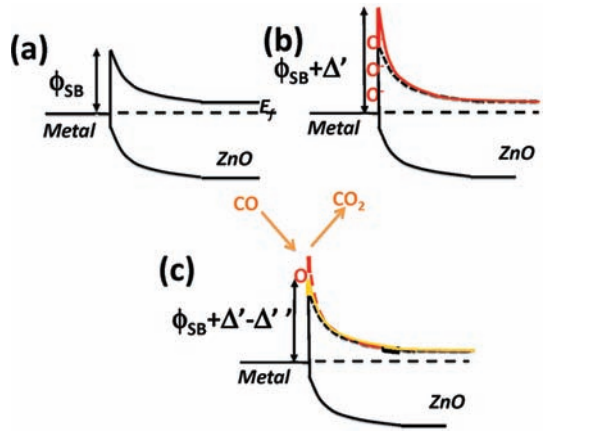

Figure 3. Proposed mechanism of the SBH variation controlled sensors. Schematics showing the response of SBH in response to variations in system atmosphere: (a) in N_2 atmosphere, (b) in O_2 atmosphere, and (c) in CO atmosphere.

current from the metallic domain (Pt) to the semiconductor domain (ZnO) under the reverse bias mode. This is also why the Schottky contact characteristics of the SCD became more pronounced upon adsorption of the oxygen ions. Figure 3a,b illustrates the SBH (φ_{SB}) rise by an amount of Δ' associated with the adsorption of O^- at the metal−semiconductor interface. The red line depicts the final band structure after the local SBH rise. This SBH rise led to more than 1 order of magnitude reduction in electric current for the SCRD, giving rise to the observed ultrahigh sensitivities.

The SBH change of the present oxygen adsorbed Schottky contact can be approximately estimated via the classic thermionic emission−diffusion theory by the following equation:[26−28]

$$\ln[I(O_2)/I(N_2)] \sim \Delta A^{**}/A^{**} - \Delta\phi_{SB}/kT \qquad (1)$$

Here, $I(O_2)$ and $I(N_2)$ are the electric currents measured at the O_2 and N_2 atmospheres at a fix voltage of −0.5 V, A^{**} is the effective Richardson constant, φ_{SB} denotes the SBH, k and T are the Boltzmann constant and system temperature, respectively. The first term on the right-hand side of the equation is negligibly small and can be safely ignored. The SBH rises thus estimated at the six different temperatures are plotted against the system temperature, as shown in Figure 4b. It is evident that the SBH rise increases with increasing temperature up to 250 °C because of the increasing amount of O^- adsorption that led to a more negatively charged state at the junction. Equation 1, however, becomes unreliable for temperatures above 250 °C since the effect of high energy electron comes into the play. Despite this incomplete information, the trend of the SBH agrees well with that of the sensitivity.

We further utilize the new device design in sensing CO, one of the toxic gases requiring high sensitivity detection. Before introducing the CO gas into the system, the device was pretreated with an O_2 atmosphere, provided by dry air. After O_2 conditioning, the system was purged with N_2 to remove the excessive O_2 remaining in the device chamber. Finally, CO gas

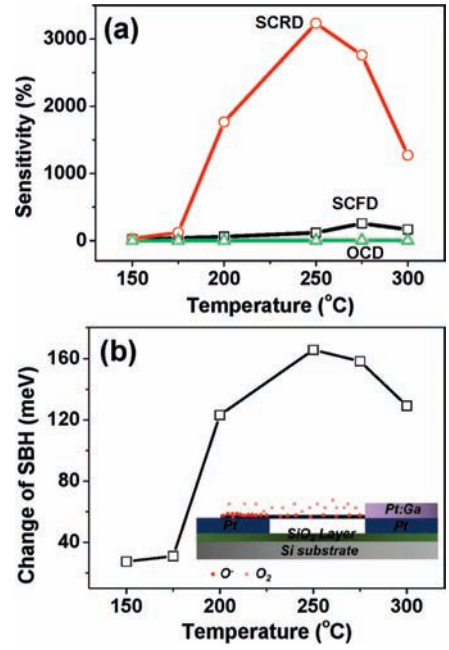

Figure 4. (a) Sensitivity versus system temperature for O_2 sensing at a response time of 500 s. Results collected from the OCD, SCD at forward bias (SCFD), and SCD at reverse bias (SCRD) were compared. (b) Derived SBH rise of the SCD at the reverse bias mode after the O_2 adsorption versus system temperature. Inset shows the schematic of the SCD at O_2 adsorption.

was introduced to the system for sensing measurements. After CO sensing for 60 min, dry air was used again as an SBH recovering gas. When using N_2 to purge the excessive O_2, the electric current would increase slightly if the system temperature was higher than 250 °C. This phenomenon may be attributed to the effect of high energy electrons and the minor desorption of O_2. This electric current pick-up during the N_2 purge, however, was insignificant and caused only very minor errors for the sensitivity calculations. The baseline currents at temperatures higher than 225 °C were measured and are shown in Figure S2h in the Supporting Information. Evidently, the current pick-up was only detectable when the temperature was higher than 250 °C and the magnitude was very small, less than 15 nA for a duration of 60 min. The baseline currents were deducted from the sensitivity calculations at these two temperatures. The response curves for the SCRD exposed to five different concentrations of CO atmospheres and measured at 275 °C are shown in Figure 5a. The blue region includes two processes: O_2 conditioning and N_2 purge. The pink region denotes the CO sensing for duration of 60 min. It was observed that the sensitivity increased with increasing concentration of CO, consistent with the theory of Scott.[29−31] The response was slow mainly because of the low reaction rate between CO and O^- to form CO_2 possibly due to the trapping effect from surface/defect states. Figure 5b shows the response curves of the OCD exposed to five different concentrations of CO atmospheres and measured at 275 °C. The current increased during the N_2 purge due to the partial desorption of O^- from the NW surface. The sensitivity of the OCD also increased with increasing CO

(26) Zhou, J.; Fei, P.; Gu, Y.; Mai, W.; Gao, Y.; Yang, R.; Bao, G.; Wang, Z. L. *Nano Lett.* **2008**, *8*, 2973.
(27) Zhou, J.; Gu, Y.; Fei, P.; Mai, W.; Gao, Y.; Yang, R.; Bao, G.; Wang, Z. L. *Nano Lett.* **2008**, *8*, 3035.
(28) Sze, S. M. *Physics of Semiconductor Devices*; John Wiley & Sons: New York, 1981.
(29) Scott, R. W. J.; Yang, S. M.; Chabanis, G.; Coombs, N.; Williams, E.; Ozin, G. A. *Adv. Mater.* **2001**, *13*, 1468.
(30) Wan, Q.; Li, Q. H.; Chen, Y. J.; Wang, T. H.; He, X. L.; Li, J. P.; Lin, C. L. *Appl. Phys. Lett.* **2004**, *84*, 3654.
(31) Wang, B.; Zhu, L. F.; Yang, Y. H.; Xu, N. S.; Yag, G. W. *J. Phys. Chem. C* **2008**, *112*, 6643.

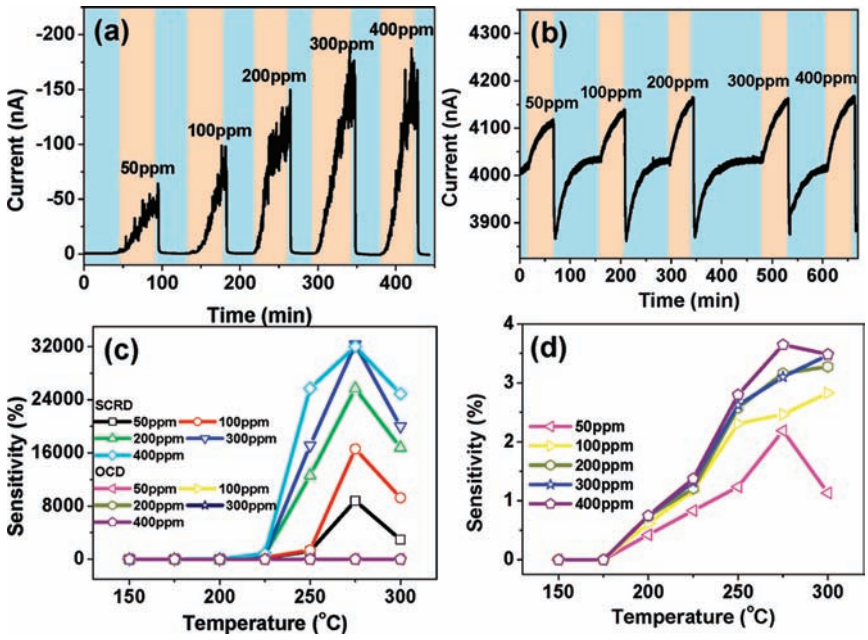

Figure 5. Response curves of the carbon monoxide detection recorded at 275 °C with the device exposed to increased concentration of CO: (a) for the Schottky contact device operated at the reverse bias mode, and (b) for the Ohmic contact device. (c) Sensitivity versus system temperature for CO sensing at a response time of 1 h as a function of the CO concentration. Results collected from the OCD and SCD at reverse bias (SCRD) are compared. (d) Enlarged plot of the data from panel (c) for the OCD.

concentration. From the response curves of Figure 5a,b, it is clear that the sensitivities of the SCRD were much higher than those of the OCD. We plotted in Figure 5c the sensitivities versus temperature for the SCRD and OCD with the CO concentration as the varying parameter. All of the relevant response curves for the CO sensing are collected in Figures S1 and S2 in the Supporting Information. The sensitivity of the SCRD was 4025 times higher than that of the OCD at a low CO concentration of 50 ppm measured at 275 °C. When the CO concentration was increased to 400 ppm at 275 °C, the sensitivity of the SCRD was further increased to 8776 times that of the OCD. A highest sensitivity of 32 000% for the SCRD was obtained at 275 °C in the CO concentration of 400 ppm. The sensitivity versus temperature plot of the OCD is displayed alone in Figure 5d to more clearly see the trends.

It is noticed in Figure 4 and Figure 5c,d that the measured sensitivity first increased with temperature, then a drop was observed with further increase of temperature. This has been suggested in the literature as the difference in activation energies related to gas adsorption and desorption. Since the desorption process requires a higher activation energy, the adsorption process is dominant at lower temperature; thus, the sensitivity increases with temperature. However, at higher temperature, the desorption process becomes dominant, which may lead to the decrease in gas sensitivity.

The ultrahigh sensitivity of the SCRD toward CO may be attributed to the variation of SBH, which is chosen to typically characterize the performance of a Schottky barrier. For simplicity of description, the barrier serves as a "gate" that controls the current to be transported. Figure 3c illustrates the relevant mechanism. At the O_2 conditioning step, the SBH was raised by an amount of Δ' via the adsorption of the negatively charged oxygen on the ZnO NW surface. Subsequently, when CO was introduced into the system, the CO combines with O^- to form CO_2. The SBH was decreased by an amount of Δ'' due to the consumption of the surface oxygen. The orange line in Figure 3c depicts the final band structure after the CO sensing. Through this SBH variation, the corresponding change in conductance can be so dramatic that ultrahigh sensitivity toward CO is achieved.

Although we have demonstrated that the SCD gives the highest sensitivity, the use of fine nanowires is indispensible. With the use of a NW, the contact area between the NW and the electrode is rather small, so that the ratio of circumference of the contact to the contact area is large, which amplifies the influence of the molecules adsorbed at the junction to the local SBH. As the total conductance is dominated by the contact inside the contact area (core area) and the areas near the outer surface, use of nanowires suppresses the relative contribution of the former.

Conclusions

A new single NW based gas nanosensor is fabricated to achieve ultrahigh sensitivities toward sensing of O_2 and CO. In contrast to the conventional sensor that utilizes Ohmic contacts, the great success of this new device relies on the modulation of the Schottky barrier height through adsorption and removal of negatively charged oxygen ions. As for the O_2 sensor, the working temperature ranges from 150 to 300 °C, in which O^- is the main state for the chemisorbed oxygen. With these negatively charged molecules adsorbed on the NW surface, including the Schottky junction, not only the charge transport through the NW is retarded because of the electron-depleted surface layer but also, more importantly, the SBH of the Schottky contact is raised;[22] the latter drastically lowers the amount of charge carrier transportable across the contact interface. Consequently, the system conductance before and after the introduction of oxygen will differ to a great extent, giving rise to high sensitivity toward oxygen detection.

This oxygen adsorbed state can be further used as a detection host for CO gas. Once CO, a toxic gas much desired to be detected, is introduced into the system, the CO would react with

the adsorbed oxygen species to form CO_2,[24] thus releasing oxygen from the NW surface. The end result is the corresponding reduction in the SBH of the Schottky contact and the electron-depleted surface layer thickness of the ZnO NW, leading to a drastic current recovery of the device, from which CO can be detected with an extremely high sensitivity. A maximum of 5 orders of magnitude improvement in CO sensing has been achieved using this new device design concept. Moreover, the response time and rest time of the nanosensor have been reduced by a factor of 7. This SBH modulation based gas sensing concept is expected to apply equally well to other gas sensing systems. The methodology and principle illustrated in the paper presents a new sensing concept that can be readily and extensively applied to other gas sensing systems.

(24) Gong, H.; Hu, J. Q.; Wang, J. H.; Ong, C. H.; Zhu, F. R. *Sens. Actuators, B* **2006**, *115*, 247.

Acknowledgment. This research was supported by DARPA (Army/AMCOM/REDSTONE AR, W31P4Q-08-01-0009), BES DOE (DE-FG02-07ER46394), the Air Force Office (FA9550-08-1-0446), DARPA/ARO W911NF-08-1-0249, the KAUST Global Research Partnership, and NSF (DMS 0706436, CMMI 0403671). The financial support provided by the National Science Council of the Republic of China (Taiwan) under Grants NSC-98-2221-E-007-034-MY3 (S.-Y.L.), NSC97-2917-I-007-108 (T.-Y.W.), and NSC98-2112-M-032-003-MY3 (P.-H.Y.) is also greatly appreciated. We also thank Dr. Qin Kuang for setting up the gas sensor measurement system.

Supporting Information Available: Response curves of carbon monoxide sensing at different temperatures and CO concentrations by the SCRD and OCD. This material is available free of charge via the Internet at http://pubs.acs.org.

JA907585C